

Fidelity of Deoxynucleic S-Methylthiourea (DNmt) Binding to DNA Oligomers: Influence of C Mismatches

Dev P. Arya and Thomas C. Bruice*

Contribution from the Department of Chemistry, University of California, Santa Barbara, California 93106

Received July 23, 1999

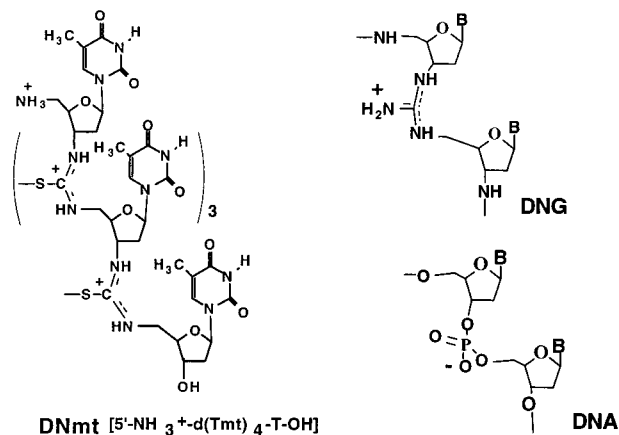
Abstract: Complementary short-strand DNA homooligomers and methylthiourea linked homonucleosides associate and form triplexes in solution. The melting temperatures, T_m , and the association and dissociation kinetic and thermodynamic parameters were determined by UV thermal analysis for the triplexes of short-strand DNA homooligomers (1-A₂₀, 2-CA₄CA₄CA₄C, 3-C₂A₃C₂A₃C₂A₃C₂, 4-C₃A₂C₃A₂C₃A₂C₂, and 5-CA-CACACACACACACACA) with the S-methylthiourea linked nucleoside {5'-NH₃⁺-d(Tmt)₄-T-OH (DNmt₅)}. Circular dichroism studies show evidence of triple-helical association dependent on the mismatch content of the target homooligomer. The melting and cooling curves exhibit hysteresis behavior in the temperature range of 10–95 °C at 0.13 deg/min thermal rate. From these curves the rate constants for association (k_{on}) and dissociation (k_{off}) were obtained. T_m decreases drastically with increase in mismatch of the target oligomer. The rate constants k_{on} and k_{off} at a given temperature (288–310 K) are dependent on the C/A ratio. The free energies of triplex formation (ΔG°) become appreciably less negative as the ratio of C to A increases. Thymidyl DNmt is shown to bind to DNA oligomers with high fidelity under physiological conditions.

Introduction

The negatively charged phosphodiester linkages of double and triple stranded DNA and RNA reside side by side causing considerable charge–charge electrostatic repulsion. This is particularly so at the low ionic strength that is physiological. This feature, as well as the susceptibility of DNA and RNA to nuclease activity, limits the usefulness of RNA and DNA as antisense or antigene drugs.^{1,2} We have reported the replacement of the phosphate linkages in DNA and RNA by achiral guanido groups, which we identify as DNG and RNG,^{3–6} and more recently have designed the polycationic nucleotide linkage with methylisothiuronium salts, or methylated thioureas, abbreviated as DNmt (Scheme 1).^{7–9} Our studies have established that d(Tmt)₄-T-OH does not form H-bonded (Watson–Crick) complexes with poly(dG), poly(dC), and poly(dU) and recent studies with the very stable (5'-NH₃⁺-d(Tmt)₄-T-OH)₂·d(pA)_x complexes warrant further investigation of DNmt oligos as sources of antisense/antigene agents.⁹

In this regard, it is important to determine if the fidelity of base recognition between phosphate-linked oligos and S-methylthiourea linked oligonucleotides is comparable to that observed in double- and triple-stranded complexes involving DNA and RNA oligomers. In this study we report the melting temperatures, T_m , as well as the association and dissociation

Scheme 1. Structures of DNmt, DNG, and DNA Linkages



Scheme 2. List of Oligomers Used in the Study

1. 5'-AAAAAAAAAAAAAAAAAAAAAAAA-3'
2. 5'-CAAAACAAAACAAAACAAA-3'
3. 5'-CCAAACCAAACCAAACCAA-3'
4. 5'-CCCAACCCAACCCAACCCA-3'
5. 5'-CACACACACACACACACACA-3'

kinetic and thermodynamic parameters for the formation of triplexes with mismatched base pairs of 20-mer DNA A_nC_n-oligomers (1–5, Scheme 2) and the S-methylthiourea (mt) linked thymidyl nucleoside, 5'-NH₃⁺-d(Tmt)₄-T-OH. Our results indicate that thymidyl DNmt binds to adenosyl DNA with remarkable fidelity with a large decrease in binding as the C content of oligos (1–5) is increased.

Experimental Section

Materials. DNmt was synthesized as previously reported.^{7,8} The concentrations of nucleotide solutions were determined using the

(1) Mesmaeker, A. D.; Haner, R.; Martin, P.; Moser, H. *Acc. Chem. Res.* **1995**, *28*, 366.

(2) Bennett, C. F. *Biochem. Pharmacol.* **1998**, *55*, 9.

(3) Browne, K. A.; Dempcy, R. O.; Bruice, T. C. *Proc. Natl. Acad. Sci. U.S.A.* **1995**, *92*, 7051.

(4) Dempcy, R. O.; Almarsson, O.; Bruice, T. C. *Proc. Natl. Acad. Sci. U.S.A.* **1994**, *91*, 7864.

(5) Dempcy, R. O.; Browne, K.; Bruice, T. C. *J. Am. Chem. Soc.* **1995**, *117*, 6140.

(6) Dempcy, R. O.; Browne, K.; Bruice, T. C. *Proc. Natl. Acad. Sci. U.S.A.* **1995**, *92*.

(7) Arya, D. P.; Bruice, T. C. *J. Am. Chem. Soc.* **1998**, *120*, 12.

(8) Arya, D. P.; Bruice, T. C. *J. Am. Chem. Soc.* **1998**, *120*, 6619.

(9) Arya, D. P.; Bruice, T. C. *Proc. Natl. Acad. Sci. U.S.A.* **1999**, *96*, 4384.

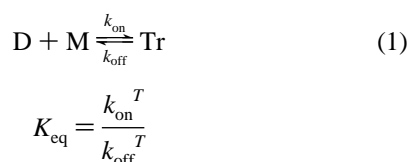
extinction coefficients (per mole of nucleotide) calculated according to the nearest neighboring effects. For d(Tmt)₅ we used $\epsilon_{268} = 8700 \text{ M}^{-1} \text{ cm}^{-1}$. All experiments were conducted in either (a) 0.015 M phosphate buffer at pH 7–7.5 or (b) 0.008 M phosphate buffer at pH 6.85. The ionic strength, μ , was adjusted with KCl and is presented with the corresponding concentration of KCl. The concentration of nucleosides, expressed in M/base, was between $1 \times 10^{-5} \text{ M}$ and $4.0 \times 10^{-5} \text{ M}$ and the ionic strength ranged from 0.03 to 0.12 M KCl. The nucleoside concentration referred to is the limiting component forming the triplex (e.g., a concentration of $4.0 \times 10^{-5} \text{ M/base}$ in the reaction of A+2T means $[A] = 4.0 \times 10^{-5} \text{ M/base}$ and $[T] = 8.0 \times 10^{-5} \text{ M/base}$). All stock solutions were kept at 4 °C between experiments.

CD, UV Spectroscopy, and Data Collection. CD spectra were obtained on an OLIS RSM circular dichroism spectrophotometer. Scans were run from 320 to 190 nm. Measurements were recorded at every nanometer. Ten scans were recorded, averaged, and smoothed for each curve. Samples were held in a 1 cm path length cuvette at 25 °C. UV spectra were recorded at $\lambda = 260 \text{ nm}$ on a Cary 1E UV/vis spectrophotometer equipped with temperature programming. Spectrophotometer stability and λ alignment were checked prior to initiation of each melting point experiment. For the T_m determinations derivatives were used. Data were recorded every 1.0 deg. The samples were heated from 25 to 95 °C at 5 deg/min (Scheme 1), the annealing (95–5 °C) and the melting (5–95 °C) were conducted at 0.13 deg/min, and the samples were brought back to 25 °C at a rate of 5 deg/min. The reaction solutions were equilibrated for 15 min at the highest and lowest temperatures.

Data Analysis. The raw data from the melting point determinations were subjected to Gaussian smoothing using Matlab 4. Calculations of kinetic/thermodynamic parameters were performed using the resulting database.

Results and Discussion

Analysis of Kinetic Data for Triplex Formation. The equation for triplex formation that was employed (eq 1



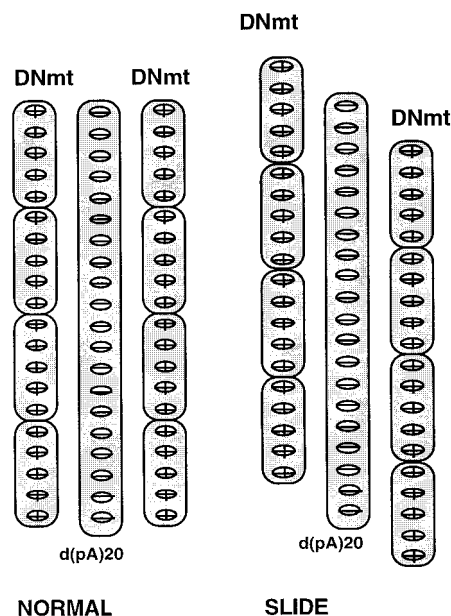
) describes the formation of the triplex (Tr) from the duplex (D) and the monomer (M), as individual strands. This equation could be interpreted as the reaction of double-strand D with single-strand M. However, the process of triplex formation may take place in different ways which we shall refer to as normal and slide (or dangling ends) (Scheme 3).^{9,10}

The expression of kinetic equations for the reactants and products (eq 2) can be accomplished by expressing the

$$\frac{d[D]}{dt} = k_{\text{off}}^T [\text{Tr}] - k_{\text{on}}^T [D][M] \quad (2)$$

concentrations of strands in molar per base (M/base). The theory behind the “on” and “off” rates of the dissociation/association of the triplexes and the derivation of kinetic equations has been described in detail.^{9–12} In eq 1, a triplex is formed from and dissociates to a duplex and a third monomer strand with rate constants k_{on} and k_{off} . The associated rate for this reaction is

Scheme 3



given in eq 2. The limitations of using this model to similar studies of $\text{DNG}_2 \cdot \text{DNA}$ triplexes have been previously discussed.^{10,11}

Letting $D_{\text{tot}} = [D] + [\text{Tr}]$ and $M_{\text{tot}} = [M] + [\text{Tr}]$, where the subscript “tot” stands for the total concentration and superscript T stands for temperature, the monitored absorbance is a weighted combination of the absorbances of the trimer, dimer, and monomer (eq 3) where $\alpha = [\text{Tr}]/D_{\text{tot}}$.

$$A = \alpha A_{\text{Tr}} + (1 - \alpha) A_{\text{D+M}} \quad (3)$$

The expressions for k_{on} and k_{off} were solved as previously reported.^{9–12} The rate constants k_{on} and k_{off} are functions of temperature and, therefore, can be expressed as Arrhenius equations:

$$k_{\text{on}} M_{\text{tot}} = k_{\text{on}}^{\text{ref}} M_{\text{tot}} \exp\left\{-\frac{E_{\text{on}}}{R} \left(\frac{1}{T} - \frac{1}{T_{\text{ref}}}\right)\right\} \quad (4a)$$

$$k_{\text{off}} = k_{\text{off}}^{\text{ref}} \exp\left\{-\frac{E_{\text{off}}}{R} \left(\frac{1}{T} - \frac{1}{T_{\text{ref}}}\right)\right\} \quad (4b)$$

where $R = 1.98 \text{ cal}/(\text{mol} \cdot \text{K})$ and T_{ref} is the reference temperature at which the rate constant k^{ref} applies. In a plot of $\ln(k_{\text{on/off}})$ vs $1/T - 1/T_{\text{ref}}$, the thermodynamic parameters $\{E_{\text{on/off}}/R\}$ can be obtained as the slope and the kinetic $k_{\text{on}} M_{\text{tot}}$, k_{off} parameter as the y intercept.

Kinetics of Triplex Association/Dissociation and Circular Dichroism Studies. An expression that provides the temperature dependence of the rate constants for association (k_{on}) and dissociation (k_{off}) of oligomeric triplex (eq 1) is provided in eq 4. As the rate of the heating and cooling increases, the rate of equilibration of the species lags such that the hysteresis becomes more marked. The four ramps depicted in Figure 1 are the variation of the absorbance (A_{260}) vs temperature. The melting temperatures, T_m , and the association and dissociation kinetic and thermodynamic parameters were determined by UV thermal analysis for the triplexes of short-strand DNA homooligomers {1–5} with the *S*-methylthiourea linked nucleoside {5'-NH₃⁺-d(Tmt)₄-T-OH (DNmt₅)}. As experienced with our previously reported studies of DNmt binding to poly(dA) and poly(rA),^{7,9}

(10) Blasko, A.; Dempcy, R. O.; Minyat, E. E.; Bruice, T. C. *Biochemistry* **1997**, *36*, 7821.

(11) Blasko, A.; Dempcy, R. O.; Minyat, E. E.; Bruice, T. C. *J. Am. Chem. Soc.* **1996**, *118*, 7892.

(12) Rougee, M.; Faucon, B.; Mergny, J. L.; Barcelo, F.; Giovannageli, C.; Garestier, T.; Helene, C. *Biochemistry* **1992**, *31*, 9269.

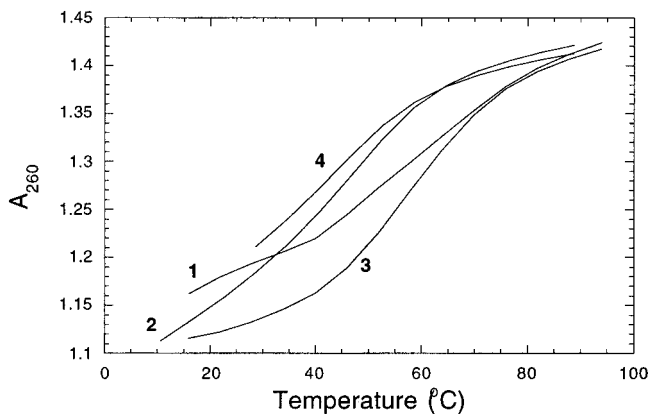


Figure 1. Effect of the heating/cooling rate on the extent of association/dissociation of the triplex of oligo **1** with 5'-NH₃⁺-d(Tmt)₄-T-OH at 4.0×10^{-5} M/base monomer concentration: (1) fast heating (5 deg/min); (2) slow annealing (0.13 deg/min); (3) slow melting (0.13 deg/min); and (4) fast cooling (5 deg/min).

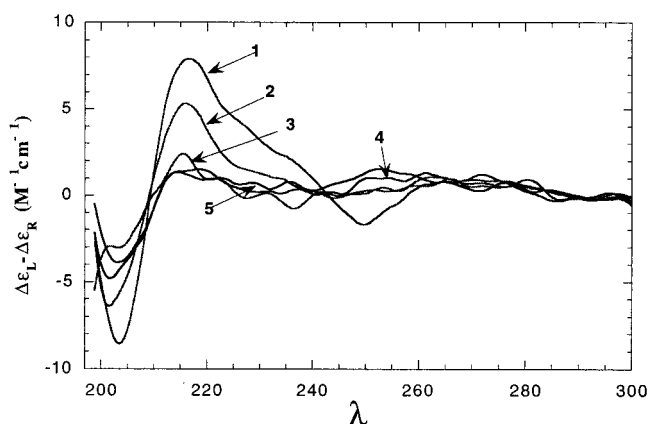


Figure 2. Difference CD spectra of oligos (**1–5**) binding to DNmt. The ratio of d(pA_xC_y) to DNmt was 1:2. Spectrum **1** refers to the difference spectra [**1** - (DNmt)₂·**1**] triplex. Solution conditions: 1.0×10^{-5} M in oligomer, 0.10 M KCl, 10 mM phosphate buffer, pH 6.8 at 25 °C.

the Job plots clearly establish a minimum at ca. 67% 5'-NH₃⁺-d(Tmt)₄-T-OH that corresponds to the formation of a 2:1 (5'-NH₃⁺-d(Tmt)₄-T-OH)₂·(DNA) complex. The hyperchromicity in binding decreased considerably on going from oligo **1** to oligo **5**. Circular dichroism studies show evidence of triple-helical association dependent on the mismatch content. The CD spectrum of an oligomer solution can give valuable information about the conformation of the oligomers as single strands or in association with other DNA oligomers. Any CD signals observed in the absorbance band of the bases (230–300 nm) are due to spatial organization of the bases in a chiral structure, such as a helix, under the influence of the chiral sugar backbone. Base stacking interactions magnify this effect and give rise to the strong CD signals observed for DNA and RNA oligomers and polymers. When DNmt is associated with complementary DNA, the CD spectrum of the complex does not match the spectrum calculated from the weighted sums of the CD spectra for the constituent oligomers. Figure 2 shows the difference spectra of 5'-NH₃⁺-d(Tmt)₄-T-OH binding to oligos **1–5**. Clear differences can be seen indicating that different degree of structural changes have taken place in the three oligomers because of their association. The negative peaks at 250 nm gradually disappear on going from oligo **1** to oligo **5** and there is considerable weakening of the positive signal at 212 nm. For the complementary d(pA)₂₀-oligo **1**, the difference spectra shows

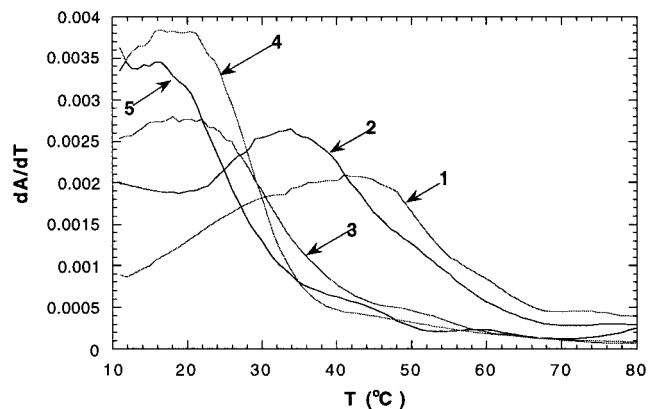
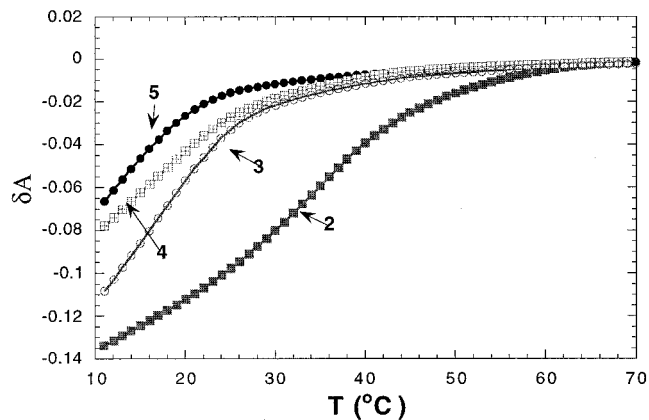


Figure 3. (a) Melting curves of the (DNmt)₂·d(pA_xC_y) triplexes (with oligos **2–5**). Solution conditions: 16×10^{-6} M in oligomer, 0.10 M KCl, 10 mM phosphate buffer, pH 6.8 at 25 °C. (b) First derivatives of the (DNmt)₂·d(pA_xC_y) triplexes (with oligos **1–5**).

the largest changes out of all the samples. As the amount of mismatch increases, difference spectra drop in amplitude indicating that the degree of association is weakening. For the noncomplementary oligomers **4** and **5**, the difference spectra are very flat indicating little association that reorganizes the bases of the nucleosides.

T_m decreases sharply with the increase in mismatch character. Figure 3a shows the melting curves and the first derivatives of DNmt triplexes with oligos **1–5**, showing the drop in T_m as the mismatch increases. On going from oligo **1** to oligo **2** (20% mismatch), T_m of the triplex drops from 48 to 39 °C and is less than 20 °C for oligos **4** and **5** (60% and 50% mismatch, respectively). The melting and cooling curves exhibit hysteresis behavior in the temperature range of 10–95 °C at 0.13 deg/min thermal rate. The heating and cooling curves were used to calculate rate constants for association (k_{on}) and dissociation (k_{off}) of triplex formation (eq 1).^{9–11} At equilibrium, both heating and cooling curves coincide satisfying the mathematical condition $d\alpha/dt = 0$ (α = fraction of duplex engaged in the triplex). Equation 4 provides k_{on}^{ref} and k_{off}^{ref} at a given reference temperature. For our studies, plots of $\ln(k)$ vs $1/T$ were found to be linear between the temperature range of 10 and 45 °C. From the intercepts of plots of $\ln(k_{on})$ and $\ln(k_{off})$ vs $1/T - 1/T_{ref}$ we obtained $k_{on}^{ref}M_{tot}$ and k_{off} , respectively. The Arrhenius plots of DNmt triplex with oligo **1–5** at a concentration of 16 μ M are shown in Figure 4a–e. The intersection of cooling $\{\ln(k_{on}M) \text{ vs } 1/T\}$ and melting $\{\ln(k_{off}) \text{ vs } 1/T\}$ curves represent the melting point of the triplex. As is evident from the figure, the intersection of the lines moves to a lower temperature on going from oligo **1** to oligo **5**, indicating the destabilization of the helix as the mismatch content is raised.

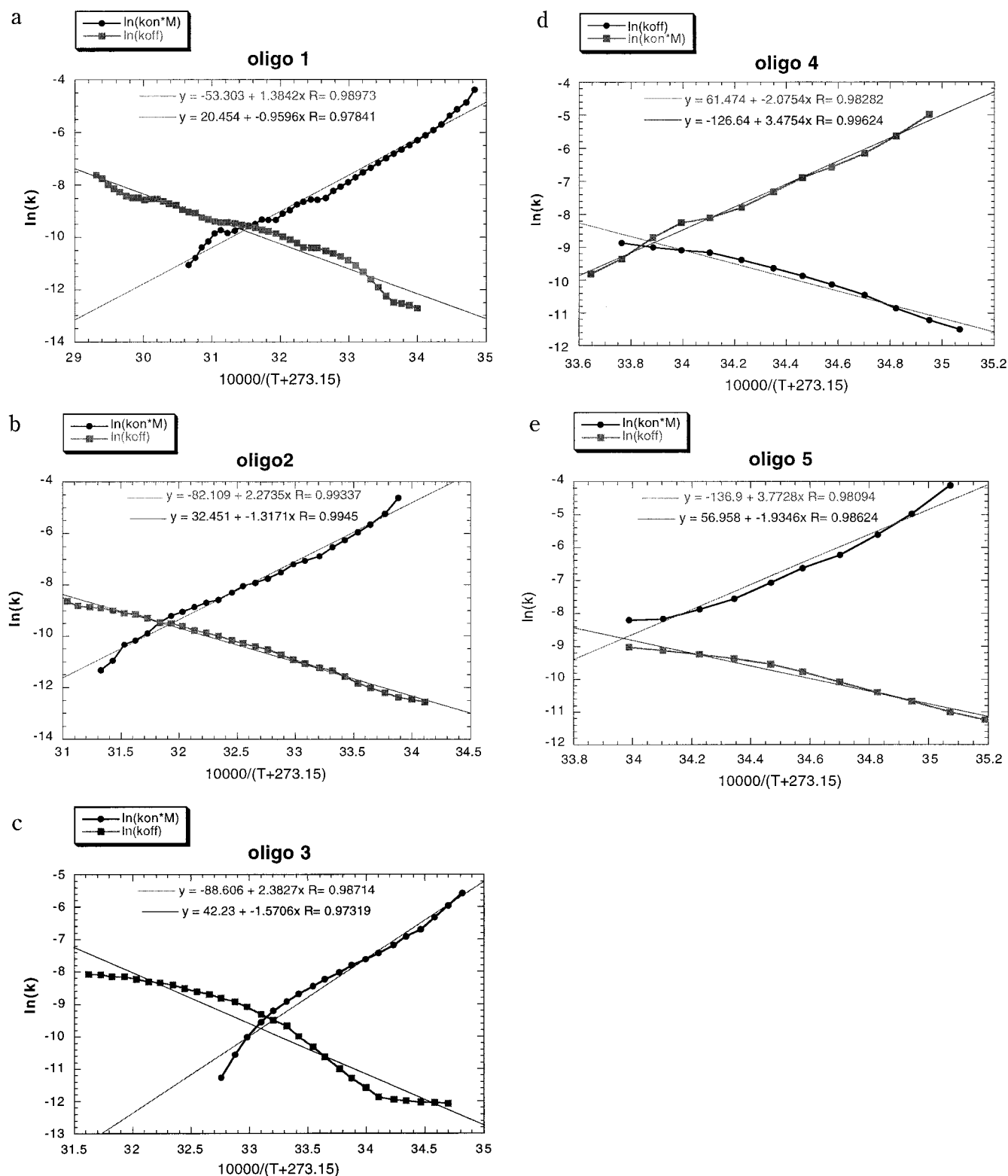


Figure 4. (a–e) Arrhenius plots $\{\ln(k) \text{ vs } 1/T\}$ for the triplexes of DNmt with oligos 1–5. Solution conditions: 16×10^{-6} M in oligomer, 0.10 M KCl, 10 mM phosphate buffer, pH 6.8 at 25 °C.

The rate constants k_{on} and k_{off} at a given temperature (288–310 K) are also dependent on the mismatch content. At physiological temperature (37 °C), k_{on} increases with decrease in mismatch whereas k_{off} decreases with increase in mismatch (Table 1). On going from oligo 1 to oligo 5, k_{on} decreases from 11.5 to $0.01 \text{ M}^{-1} \text{ s}^{-1}$ and k_{off} increases from 2.7×10^{-5} to $445 \times 10^{-5} \text{ s}^{-1}$. The free energies of formation get less negative as the mismatch content increases and become positive for oligos 4 and 5, as the duplex becomes the more stable species (T_m for

4 and 5 is less than 20 °C, implying complete dissociation of the triplex at 37 °C). At lower temperatures (15 °C), there seem to be nonspecific electrostatic interactions which seem to stabilize DNmt triplex with oligo 2 more than oligo 1. On going to oligos 3–5, however, stability of the triplex decreases considerably, as expected from specific H-bonded triplex formation. For example, at 15 °C, $\Delta\Delta G_{(1-5)}$ for triplex formation is 2.2 kcal/mol compared to $\Delta\Delta G_{(1-5)}$ of 7.3 kcal/mol at 37 °C. Oligo 4 (60% C) forms a slightly more stable triplex (by

Table 1. Melting Points (T_m), Rates of Association (k_{on}) and Dissociation (k_{off}) of DNmt Triplexes with $d(pA_xC_y)$ Oligomers **1–5**, and Free Energies of Formation of $d(pA_xC_y) \cdot (DNmt)_2$ Triplexes at 15 and 37 °C^a

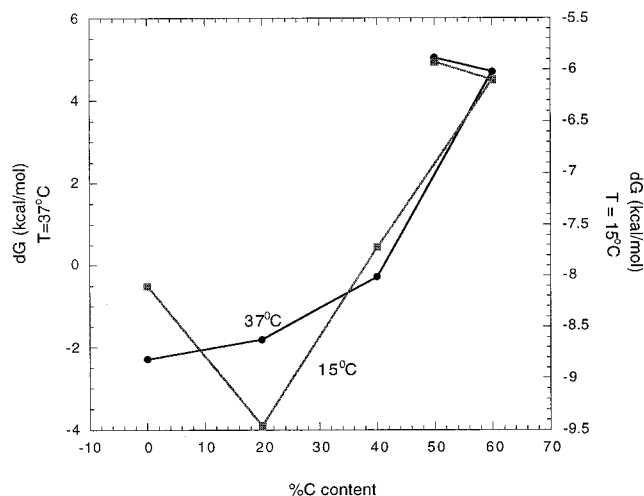
oligo	T_m (°C)	T (°C)	$10^4 k_{on} M$ (s ⁻¹)	$10^6 k_{off}$ (s ⁻¹)	$10^{-2} K_{eq}$	ΔG (kcal/mol)
1	48.1	37	1.84	27.7	41.5×10^2	-2.3
2	39.0	37	1.36	44.5	19.2×10^2	-1.8
3	25.6	37	5.60×10^{-1}	2.24×10^2	1.57×10^2	-3.0×10^{-1}
4	19.9	37	3.00×10^{-3}	43.3×10^2	5.0×10^{-2}	4.7
5	16.1	37	2.00×10^{-3}	44.5×10^2	3.0×10^{-2}	5.0
1	48.1	15	30.4	4.70	14.7×10^3	-8.1
2	39.0	15	1.52×10^2	2.20	15.9×10^4	-9.5
3	25.7	15	21.4	6.51	7.57×10^3	-7.7
4	19.9	15	13.0	68.1	4.39×10^2	-6.0
5	16.1	15	9.9	70.5	3.25×10^2	-5.9

^a The data shown are average of the values in concentration range (10 to 40 μ M) at 0.10 M KCl. Margin of error: $k_{on} M_{tot} = +0.24 \times 10^{-4} s^{-1}$, $k_{off} = +0.24 \times 10^{-6} s^{-1}$, $\Delta G = +0.2$ kcal/mol, $T_m = +1$ °C.

0.33 kcal/mol at 37 °C and by 0.2 kcal/mol at 15 °C, margin of error being 0.2 kcal/mol, $\Delta T_m = 3.9$ °C) compared to oligo **5** (50% C, alternating A and C). The plots of change in free energy with variation in mismatch content at different temperatures are shown in Figure 5 and illustrate the loss of stability of the DNmt₂·DNA triple helices complexed with noncomplementary oligos **2–4**.

The k_{on} values for the formation of DNmt₂·DNA triple helices, on average, have been found to be⁹ 1 order of magnitude larger than those found for a DNA triplex having the length of 22 bp at $[NaCl] = 0.02–0.30$ M.^{12,13} The increase in k_{off} values on increasing the mismatch content parallels the increase observed for DNA·DNA₂ triple helices.¹² On the other hand, the decrease in k_{on} values upon increase of mismatch (% C) is in contrast to that observed for DNA·DNA₂ triple helices (no change in k_{on} values was observed with the mismatch oligos in that study).¹² These comparisons are only qualitative since the ionic strength acts in the opposite direction for DNmt relative to DNA and the composition of the 22-mer DNA oligonucleotide differs from the short-strand DNA oligonucleotides in this study.

(13) Manzini, G.; Xodo, L. E.; Gasparato, D. *J. Mol. Biol.* **1990**, *213*, 833.

**Figure 5.** Plots of variation of free energies (15 °C and 37 °C) of formation of the (DNmt)₂·d(pA,C_y) triplex with increase in mismatch (% C) of oligos **1–5**.

In conclusion, the polycation 5'-NH₃⁺-d(Tmt)₄-T-OH binds to homooligomers d(pA)_x with high affinity and with base-pair specificity to provide triple-stranded helices. The electrostatic attraction between polycation 5'-NH₃⁺-d(Tmt)₄-T-OH and polyanion d(pA)_x stabilizes the triple helical hybrid structures. The free energies of triplex formation (ΔG°) become appreciably less negative as the ratio of C to A increases (oligos **1** to **5**). T_m of the DNmt₂·DNA triple helices decreases sharply with the increase in mismatch character. Thymidyl DNmt is thus shown to bind to DNA oligomers with high fidelity under physiological conditions. Synthetic efforts to design longer DNmt sequences, coupled with studies of DNmt_n·DNA complexes involving complementary and mismatch sequences, should help in further development of this novel class of putative antisense/antigene agents.

Acknowledgment. This work was supported by a grant from the National Institutes of Health (Grant No. BK09171).

JA9928711